

A Phase Model of Temperature-Dependent Mammalian Cold Receptors

Peter Roper

Paul C. Bressloff

*Nonlinear and Complex Systems Group, Department of Mathematical Sciences,
University of Loughborough, Loughborough, Leicestershire, U.K.*

André Longtin

Département de Physique, Université d'Ottawa, Ottawa, Ontario, Canada K1N 6N5

We present a tractable stochastic phase model of the temperature sensitivity of a mammalian cold receptor. Using simple linear dependencies of the amplitude, frequency, and bias on temperature, the model reproduces the experimentally observed transitions between bursting, beating, and stochastically phase-locked firing patterns. We analyze the model in the deterministic limit and predict, using a Strutt map, the number of spikes per burst for a given temperature. The inclusion of noise produces a variable number of spikes per burst and also extends the dynamic range of the neuron, both of which are analyzed in terms of the Strutt map. Our analysis can be readily applied to other receptors that display various bursting patterns following temperature changes.

1 Introduction ---

Bursting is the rhythmic generation of several action potentials during a short time, followed by a period of inactivity. The limiting case of a single spike per burst is termed *beating*. There are a wide variety of burst phenomena, but it appears that many are due to a similar underlying mechanism. The various chemical and electrical dynamics of the neuron operate on many timescales, and in some cases, the full dynamics can be dissected into a fast system coupled to a slowly oscillating subsystem (Rinzel & Lee, 1987). Typically the fast system operates on a millisecond timescale and models the currents associated with spike generation, while the slow subsystem, with a timescale of up to 1 second or more, is often associated with calcium concentrations. The fast system is modulated by the slow one and has two parameter regimes: a stationary state or “fixed point” and a limit cycle state during which action potentials are periodically generated. Thus, for this “slow-wave” bursting to occur, the slow variable must parameterize bifurcations in the fast system.

Cold receptor neurons are free nerve endings (Schäfer, Braun, & Rempe, 1990) that transduce local temperature information into neuronal signals. Their neuronal discharge takes the form of regular bursts, phase-locked single spikes ("beating"), or stochastically phase-locked spikes ("skipping"). The cells are subcutaneous to the skin and tongue but are sparsely distributed (Ivanov, 1990). Due to their small size, they cannot be recorded intracellularly, and the only quantity that can be measured directly is the spike train. However, other cellular properties may be inferred by the use of pharmacological agents. Temporal firing patterns and interspike interval histograms (ISIH) from these neurons (see Figure 1) show that the bursting dynamics is highly temperature dependent and further suggest the existence of a slowly oscillating current with a frequency that increases with temperature (Braun, Schäfer, & Wissing, 1990).

In this article we present a canonical model for a thermoresponsive cold receptor with noise that exhibits bursting, beating, and skipping. Our model is a simplified version of a full ionic model of a slow-wave burster, such as Plant's model, which formed the basis of a recently proposed model of cold thermoreception (Longtin & Hinzer, 1996). The simplified model derives from the ionic model by means of a phase-reduction procedure due to Ermentrout and Kopell (1986). Although we focus specifically on cold receptors, the phase-model approach is general and is applicable to any thermosensitive neuron that discharges in a similar manner to cold receptors (for example, certain cells exhibit similar patterns but in a different order; (Braun, Schäfer, Wissing, & Hensel, 1984). It is also applicable to other more recently proposed ionic models of cold receptors (Braun, Huber, Dewald, Schäfer, & Voigt, 1998). The model contains biologically motivated parameters and exhibits behavior that is consistent with experiment. Moreover, it has the advantage of being mathematically tractable so that if these parameters were to be quantified, analytic predictions about the behavior of real receptors could be made.

We analyze the model in the limiting case of zero noise (the deterministic limit) and also when subjected to noise originating primarily from conductance fluctuations and electrogenic pumps. For the deterministic case, we are able to predict how many action potentials are generated per burst for a given temperature and derive the transition temperature from bursting to beating. For the latter we are able to estimate the skipping rate at a given temperature. We demonstrate that skipping is a noise-induced effect that can occur for both the suprathreshold and the subthreshold dynamics. Above threshold, spikes become deleted as a consequence of noise-induced trapping (Apostolico, Gammaitoni, Marchesoni, & Santucci, 1994), while below threshold, the firing pattern becomes augmented by noise-induced spiking.

The article is organized as follows. Section 2 is a brief review of cold receptor physiology, a subject covered more completely in Longtin and Hinzer (1996). Our model is introduced in section 3. In section 4 we consider the

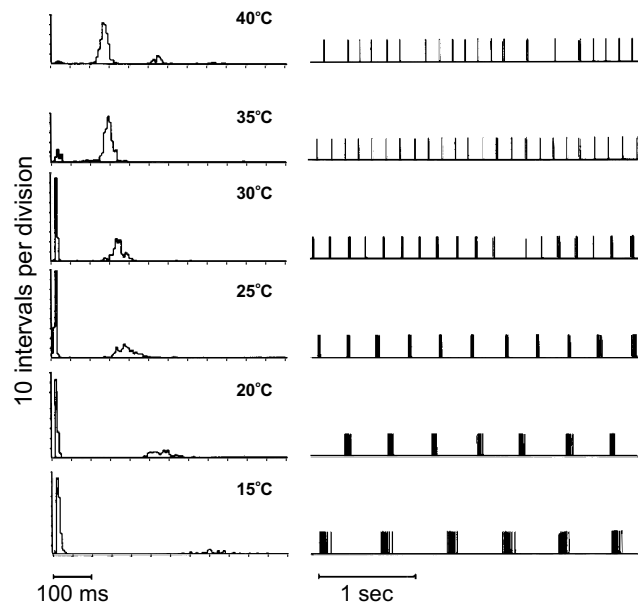


Figure 1: Characteristic discharge patterns of bursting cold receptors of the cat lingual nerve at different constant temperatures. The steady-state patterns are recorded at least two minutes after each 5°C temperature change (from Figure 1 of Schäfer et al., 1988, reproduced with permission).

limiting case of zero noise and analyze the simulated firing patterns using Floquet theory. We then examine how noise can alter the deterministic discharge pattern.

2 A Summary of the Neuro- and Electrophysiology of Cold Receptors —

Figure 1 shows characteristic discharge patterns and their associated ISIH, measured from cold receptors in a cat tongue at various static temperatures. Not every cell has this repertoire; some exhibit only a few of these patterns when the temperature is varied. Furthermore, the temperature at which a given discharge pattern occurs varies between receptors. It has been argued (Dykes, 1975) that by using the temporal structure of the discharges, the central nervous system is able to discriminate between firing patterns that have the same mean firing rate but correspond to different temperatures. This is plausible because bursts can drive higher neurons efficiently (Lisman, 1997): the relatively high firing rates during a burst release higher levels

of transmitter than would be the case if the individual spikes were more broadly distributed in time.

At low temperatures, the neuron bursts repetitively with a uniform burst length and with bursts that appear to be synchronized with some underlying slow oscillation. However, the timing of individual spikes within the burst is nonuniform (Braun, Bade, & Hensel, 1980), since the firing frequency within a burst increases. This is a feature shared with parabolic bursting neurons (Rinzel & Lee 1987).¹ When the temperature is quasi-statically increased, the burst length and interburst period diminish, until at the middle of its operating range, the neuron emits a regular spike train with phase-locked spikes.

If the temperature is increased still further, the spike train becomes aperiodic so that occasional double spikes appear and skipping occurs. The spike train is still synchronized to some underlying rhythm, but between spikes a random integer number of oscillation cycles may be skipped (Braun et al., 1990). The origin of this randomness is uncertain, but due to the cell's lack of synapses and its small size, it is thought that thermal, conductance, and other fluctuations might be important. It has been argued (see Longtin & Hinzer, 1996, for a review), based on physiological and pharmacological studies, that the key ingredients of this skipping are noise and a slow internal oscillation with a maximum amplitude that lies close to the spiking threshold. The skipping rate is also thermally dependent, increasing with temperature, and above 40°C, skips of up to eight cycles have been observed (Schäfer, Braun, & Rempe, 1988).

We introduce some nomenclature for describing the discharge pattern. The number of action potentials in a given burst is N , and the mean number of spikes per burst, \bar{N} , is the temporal average of N . Ω is the frequency of the slow oscillatory cycle and is the reciprocal of the sum of the inter- and intraburst durations. At a fixed temperature, the number of spikes per burst for a given receptor can vary by one or two (Braun et al., 1980), implying that the bursting dynamics also has a degree of stochasticity. This further suggests the presence of noise or chaos, or both (Longtin & Hinzer, 1996). The breadth of the ISIH peak corresponding to the interburst period suggests fluctuations in the slow-wave frequency $\Omega(T)$, the mean of which is determined only by T . The variability in the number of spikes per burst further contributes to this breadth. Examination of the spike trains of several cells at different static temperatures reveals (Braun et al., 1984) that both Ω and \bar{N} depend monotonically (and sometimes approximately linearly (Braun et al., 1980) on the temperature T , with Ω increasing and \bar{N} decreasing with T .

¹ A burst is termed parabolic if the spiking frequency is lower at both the beginning and the end of the burst compared with that during the middle of the burst; thus, here we have only half of the "parabolic" bursting

The thermosensitivity and regular discharge of cold receptors have been likened to that of *Aplysia* R15 neurons. Intracellular recordings of R15 have revealed the mechanism of slow-wave bursting and have shown the presence of an underlying slow-wave voltage oscillation that persists even when spike generation is pharmacologically blocked. The rhythmic behavior of *Aplysia* is well reviewed in (Canavier, Clarke, & Byrne, 1991). The thermosensitivity of *Aplysia* R15 cells has been investigated (Carpenter, 1967) (reviewed in Longtin & Hinzer, 1996), and it points to the importance of the thermosensitivity of their electrogenic ionic pumps (such as $\text{Na}^+\text{-K}^+$ ATPase); such pumps have also been found in cold receptors. It has thus been proposed that the mechanisms of bursting and thermosensitivity for both cold receptors and for *Aplysia* R15 neurons are related (Willis, Gaubatz, & Carpenter, 1974; Wiederhold & Carpenter 1982). That hypothesis was further substantiated in a recent study (Longtin & Hinzer, 1996) that extended the Plant model (Plant, 1981), devised originally for R15 bursting, to explain cold receptor firing.

Finally, skipping occurs in other preparations in which there is no apparent periodic stimulation. For example, a related thermoresponsive preparation is the ampullae of Lorenzini of the dogfish. These mandibular sensory afferents exhibit a similar temperature-dependent slow wave, but although skipping occurs, they do not burst in the same manner. Recent data (Braun, Wissing, Schäfer, & Hirsch, 1994) point to this skipping as being a consequence of noise internal to the neuron, following a mechanism similar to that suggested for cold receptors (Braun et al., 1980): a slow oscillation periodically brings the membrane potential close to the firing threshold, at which point action potentials are caused randomly by noise pushing the potential over threshold.

All of these studies suggest the following scenario. At low temperatures, the membrane potential is high and the slow wave depolarizes the membrane for a significant part of the cycle; the neuron therefore bursts. As the temperature increases, so does the oscillation frequency of the slow wave. In addition the mean potential becomes more negative (due to the electrogenic pump), and so the depolarization time due to the slow wave, and hence the burst length, is reduced. At high temperatures, the slow wave is no longer able to generate spikes by depolarization; instead, all spikes must be noise driven.

3 Temperature-Dependent Phase Model of Cold Receptor Function

3.1 A Phase Model. Plant's model (1981) of slow wave, parabolic bursting, extended to cold receptors in Longtin and Hinzer (1996), is based on a Hodgkin-Huxley-type ionic current description. Although such ionic models (see also Braun et al., 1998) elucidate cellular function, they involve many coupled differential equations and so are difficult to treat analytically. They also involve many parameters that are currently inaccessible

to experimental determination. Consequently, we seek a simpler canonical model. We write the vector of potentials and gating variables associated with spiking (e.g., fast sodium/calcium and potassium channels) as $\mathbf{u} \in \mathbb{R}^p$, and the vector of concentration and gating variables associated with the slow dynamics (e.g., calcium concentration) as $\mathbf{v} \in \mathbb{R}^q$. Ermentrout and Kopell (1986) studied parabolic bursting models with the general form

$$\begin{aligned}\dot{\mathbf{u}} &= f(\mathbf{u}) + \varepsilon^2 \mathbf{g}(\mathbf{u}, \mathbf{v}, \varepsilon) \\ \dot{\mathbf{v}} &= \varepsilon h(\mathbf{u}, \mathbf{v}, \varepsilon)\end{aligned}\tag{3.1}$$

for which the following two properties hold:

1. When $\varepsilon = 0$ the system $\dot{\mathbf{u}} = f(\mathbf{u})$ has an attracting invariant circle and a single degenerate critical point; the system is at a saddle-node bifurcation on a limit cycle.
2. $\dot{\mathbf{v}} = h(0, \mathbf{v}, 0)$ has a limit cycle solution.

They showed that such models converge in the weak-coupling limit, $\varepsilon \rightarrow 0$, to the canonical form

$$\begin{aligned}\dot{\phi} &= [1 - \cos(\phi)] + [1 + \cos(\phi)] g(0, \mathbf{v}, 0) \\ \dot{\mathbf{v}} &= \frac{1}{c} \bar{h}(0, \mathbf{v}, 0),\end{aligned}\tag{3.2}$$

where c is some constant and $f()$, $g()$, $h()$, and $\bar{h}()$ are smooth functions of their arguments. $\phi \in [-\pi, \pi]$ is defined on the unit circle S^1 and represents the phase of the membrane potential at the trigger zone. A full rotation of ϕ corresponds to the generation of an action potential.

The requirement of weak coupling ($\varepsilon \rightarrow 0$) implies that the time constants for the slow dynamics must be much smaller than those for the fast subsystem. For real cold receptors, ε is not quantifiable since there are no intracellular recordings. However, we previously (Longtin & Hinzer, 1996) proposed that the Plant model might well describe cold receptors and for this model, the coupling between fast and slow subsystems is indeed weak (Rinzel & Lee, 1987). However, as it stands, the Plant model fails to satisfy the second hypothesis since the slow subsystem approaches a fixed point when the membrane potential is clamped to any fixed value. Soto-Treviño, Kopell, & Watson (1996) have therefore generalized Ermentrout and Kopell's (EK) phase reduction and furthermore have taken the Plant model as their specific example. They show that hypothesis (2) can be replaced by the more lax criterion that there be a slow periodic orbit that remains close to a curve of degenerate homoclinic points for the fast system. Under such constraints, the Plant model may be reduced to the canonical form in equation 3.2.

We will modify the canonical form to account for temperature effects, while retaining similar dynamics and bifurcations. As a first step, we write the slow dynamics as the sum of a constant term X and a zero-mean periodic term $Y(\Omega, t)$ that oscillates with frequency Ω , and for convenience we set $\theta = \phi + \pi$. Thus

$$\dot{\theta} = [1 + \cos(\theta)] + [1 - \cos(\theta)][X + Y(\Omega, t)]. \quad (3.3)$$

In the absence of any electrophysiological evidence, we initially choose to model the oscillatory component with a simple cosine where the upward trend might derive from an inward Ca^{2+} current while the downward trend could be a Ca^{2+} -dependent outward K^+ current. Furthermore, we rescale time so that $t' = (1 - X)t$, and introduce

$$b = \frac{1 + X}{1 - X} \quad \text{and} \quad A \cos(\Omega t') = -\frac{Y(\Omega, t)}{1 - X}. \quad (3.4)$$

Thus we obtain

$$\begin{aligned} \frac{d\theta}{dt'} &= [b + \cos(\theta)] - A \cos(\Omega t') [1 - \cos(\theta)] \\ &= [b - A \cos(\Omega t')] + [1 + A \cos(\Omega t')] \cos(\theta). \end{aligned} \quad (3.5)$$

The parameter b modulates the mean potential of the cell (and hence its excitability), and thus could be associated with the activity of one or more electrogenic pumps that move ions against their concentration gradients.²

The phase model in equation 3.5 displays a saddle-node bifurcation on a limit cycle whenever

$$b - A \cos(\Omega t) = 1 + A \cos(\Omega t). \quad (3.6)$$

Time appears here explicitly (for clarity we have omitted the prime), and so for certain parameter values, the bifurcation occurs periodically in one direction followed by the other. If the slow oscillation is of such magnitude that for part of the cycle

$$A \cos(\Omega t) < \frac{(b - 1)}{2} - \eta, \quad (3.7)$$

where η is some small positive parameter, then the neuron bursts. This oscillatory behavior across the saddle node is much simpler than the corre-

² Kopell and Ermentrout (1986) discuss other possible biological correlates of the slow oscillation and make the alternative suggestion that they could derive solely from oscillations in pump activity.

sponding bifurcations undergone by ionic models. For example, the Plant model has a two-dimensional slow subsystem that depends on the three-dimensional fast subsystem, with the result that the latter is periodically driven through homoclinic transitions between steady-state and limit-cycle solutions.

Close to the bifurcation the phase model exhibits critical slowing down; relaxation to a fixed point (the resting potential) becomes polynomial in time rather than exponential, thus increasing the time for $\theta(t)$ to traverse the unit circle. Such behavior has also been described as passage through a bottleneck (Strogatz, 1994). Therefore, within a burst there is a nonuniform distribution of spikes: a signature of parabolic bursting.

Equation 3.5 may be made more tangible by graphing $1 + A \cos(\Omega t)$ and $b - A \cos(\Omega t)$, as in Figure 2a. A saddle-node bifurcation occurs when the sinusoids cross, and hence bursting occurs. The mean number of spikes per burst, \bar{N} , is proportional to Δ , the overlap of the two curves. Δ is a function of all of A , Ω , and b , and is approximated by

$$\Delta = \frac{2}{\Omega} \left(\pi - \cos^{-1} \left(\frac{b-1}{2A} \right) \right) = \frac{1}{\Omega} \left(\pi + \frac{b-1}{A} \right) + O \left[\left(\frac{b-1}{2A} \right)^3 \right]. \quad (3.8)$$

3.2 Modeling Temperature Dependence and Fluctuations. The main effect of a temperature change is a variation in the rate constants of the biochemical processes occurring within the cell. Therefore, to obtain expressions for the variation with temperature of the coefficients of the phase model, we must first consider the thermal dependence of the parameters of more biophysical models of slow-wave bursting. In the appendix, we derive a novel relationship between the frequency Ω of the slow wave in equation 3.5 and parameters of the Plant model extended to cold receptors (Longtin & Hinzer, 1996). The two main temperature-dependent parameters of the slow subsystem in the Plant model are the (positive) kinetic rates λ and ρ of, respectively, the slow inward current gating variable and the calcium dynamics. We find that $\Omega \approx (\lambda\rho)^{1/2}$.

Also, numerics suggest that the transition from fixed point to the slow-wave limit cycle is a supercritical Hopf bifurcation and that the limit cycle frequency does not depend strongly on the bifurcation parameter, as is usually the case in the vicinity of this kind of bifurcation. If both of these rates are assigned the same temperature dependence as in Longtin and Hinzer (1996)—the same Q_{10} —then Ω will vary with temperature according to this Q_{10} as well. For $Q_{10} = 3$ in Longtin and Hinzer (1996), this means that $\Omega \approx 3^{0.1T}$. This functional form readily fits the temperature dependence seen in the conductance-based model (Longtin & Hinzer, 1996) (not shown). Further, since this form is almost linear over the temperature range of interest, it is similar to the experimental observation (Braun et al., 1980) that the burst frequency (slow-wave frequency) increases linearly with T . Over a temper-

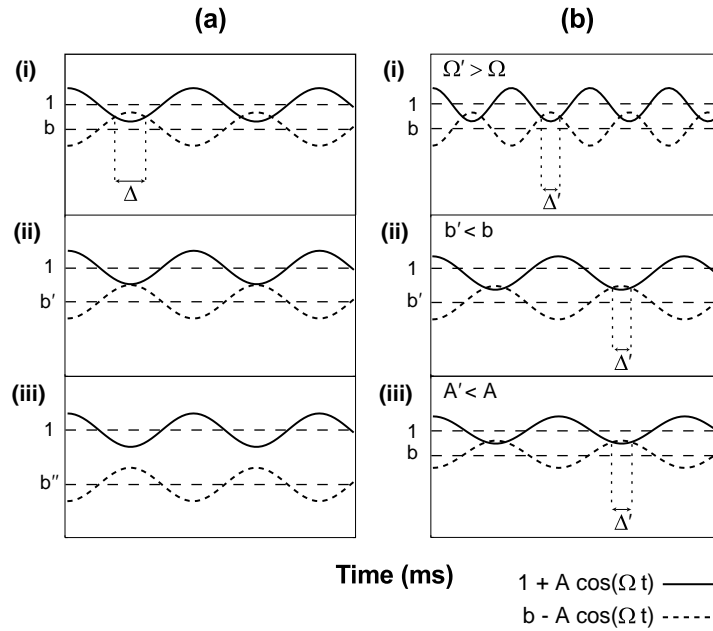


Figure 2: (a) Saddle-node bifurcation and bursting criteria for three different parameter regimes, with $b_1 > b_2 > b_3$, and $b_2 = 1 - 2A$. (i) When the overlap is large, the neuron bursts (fires repetitively) for a time Δ . (ii) Bursting has ceased; any spiking activity must be noise driven and the neuron skips (it does not always fire at every slow wave cycle). (iii) All spiking has ceased, and the neuron is silent. (b) There are three possible mechanisms by which the burst length can be reduced ($\Delta' < \Delta$) (compare with (a)): (i) increasing slow-wave frequency, $\Omega' > \Omega$, (ii) decreasing pump parameter $b' < b$, and (iii) decreasing slow-wave magnitude, $A' < A$.

ature range of 17.8° to 40°C , our analysis produces a factor 11.5 increase in frequency, which is close to the factor of 10.0 obtained from numerical simulations of the full model, and close also to actual ratios exhibited by some cold fibers.

Further bifurcation analysis could be done to compute the leading-order term for the temperature dependence of the slow-wave amplitude $A(T)$ and thus also to relate the amplitude parameter in the phase model to biophysical parameters of a conductance-based ionic model. Because we are interested only in reproducing qualitative features of thermosensitivity, we model thermal dependence with linear functions of the magnitude of the

pump coefficient, b , and of the magnitude, A , and frequency, Ω , of the slow wave.

$$b \rightarrow b(T) = b_0 - b_T T \quad A \rightarrow A(T) = A_0 + A_T T \quad \Omega \rightarrow \Omega(T) = \Omega_0 + \Omega_T T, \quad (3.9)$$

where $\Omega_0, \Omega_T, A_0, A_T, b_0$, and b_T are constants. More complex relationships could be used if required. Figure 2b shows how the individual variation of each of these parameters can alter the burst length; it is likely that the discharge patterns observed are due to some combination of these mechanisms. We furthermore confine our interest to the temperature range for which $A(T), \Omega(T) > 0$.

Neuronal noise has many possible sources and is generally difficult to measure, a problem exacerbated by the lack of intracellular recordings from these neurons. In the absence of synaptic input, its main components are due to thermal ionic movement, conductance fluctuations in the ion channels, and electrogenic pump noise (DeFelice, 1981). Thermal noise is proportional to the absolute temperature, and so varies only slightly over the temperature range of interest.

For simplicity again, we lump noise terms together into an additive noise on the θ dynamics (see equation 3.5), as previously proposed in Longtin and Hinzer (1996) (and references therein). We further assume that the noise $\xi(t)$ has a zero-mean gaussian distribution and is white:

$$\langle \xi(t) \rangle = 0 \quad \text{and} \quad \langle \xi(t) \xi(t') \rangle = 2D \delta(t - t'). \quad (3.10)$$

We refer to the noise variance $D = \sigma^2$ as the noise strength. Thus we write

$$\frac{d\theta}{dt} = b(T) - A(T) \cos(\Omega(T)t) + [1 + A(T) \cos(\Omega(T)t)] \cos(\theta) + \xi(t). \quad (3.11)$$

From now on, $b(T)$, $A(T)$, and $\Omega(T)$ are assumed to depend implicitly on temperature.

If we now examine the system numerically for different temperatures (see Figure 3) and choose b_0, b_T, A_0 , and A_T such that at low temperatures there is a part of the cycle for which equation 3.7 is satisfied, then we observe that the neuron bursts (see the inset to Figure 3f). As T increases, $\Omega(T)$ and $A(T)$ both increase while $b(T)$ decreases. However, for a given temperature change, the increase in $A(T)$ is smaller than and is counteracted by the larger change in $b(T)$. In this way both the intra- and interburst periods also decrease with temperature (see the insets to Figures 3d and 3e). We thus obtain a sequence of firing patterns similar to that seen experimentally (see Figure 1). At low temperatures, bursts are lengthy, and so the dominant component of the ISIH is a narrow peak close to the origin (see the inset to Figure 3f), which corresponds to the timing of successive spikes in a burst (the intraburst period). As the temperature increases, the burst length decreases and the

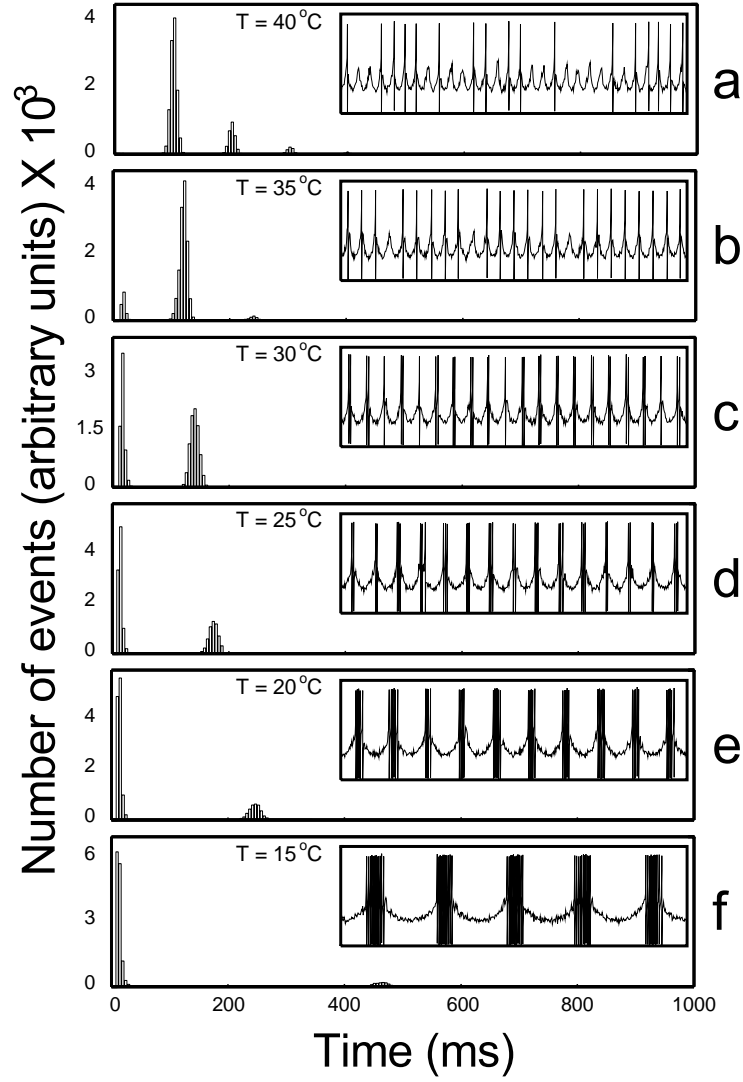


Figure 3: Simulated spike trains (inset figures) and corresponding interspike interval histograms (main figures) for increasing temperatures. Parameters are: $A_0 = 0.3$, $A_T = 0.001$, $b_0 = 0.675$, $b_T = 0.007$, $\Omega_0 = -\pi/150$, $\Omega_T = \pi/1500$, and $D = 0.05$.

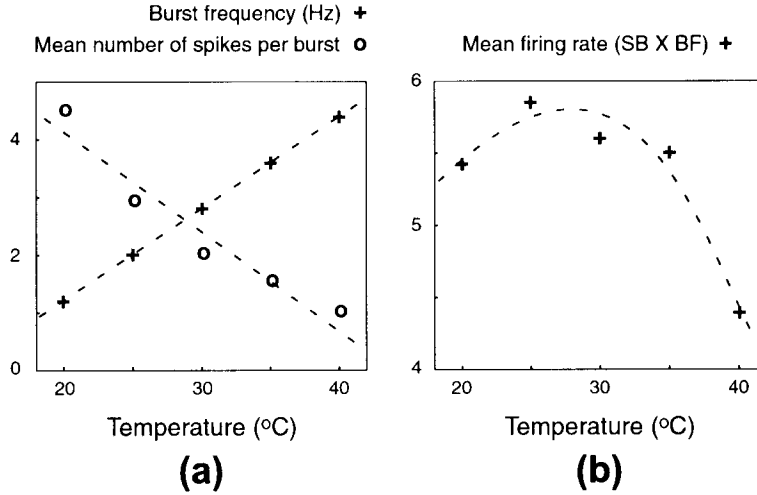


Figure 4: Cold receptors encode temperature by means of their firing patterns and not by a mean rate code. The efficiency of this strategy is shown by their ability to encode two different temperatures with the same mean firing rate: (a) The variability with temperature of the number of spikes in a burst (SB) and the burst frequency (BF). (b) The mean firing rate (BF \times SB) varies with increasing temperature. See Figures 10a and 10b of Braun et al., (1980). Parameters are: $A_0 = 0.234$, $A_T = 0.0004$, $b_0 = 0.5868$, $b_T = 0.00088$, $\Omega_0 = -\pi/150$, $\Omega_T = \pi/3000$, and $D = 0.025$.

interburst period becomes a pronounced feature of the ISIH: a new peak appears close to one period of the slow-wave oscillation (see Figures 3b and 3c). For high T equation 3.7 is never satisfied, and bursting does not occur; instead, all spikes are noise driven (see the insets to Figures 3a and 3b) and higher subharmonics of the slow wave begin to appear in the ISIH.

Furthermore, our canonical model can encode two different temperatures by two different firing patterns that have the same mean firing rate, as shown in Figure 4 (cf. Figures 10a and 10b of Braun et al., 1980).

4 Analysis of Bursting and Beating

The neuron's behavior depends sensitively on both the noise strength and the temperature. If we graph the mean number of spikes per burst, $\bar{N}(T)$, versus T for a neuron subject to a vanishingly small level of noise, we observe the staircase depicted in Figure 5. Note that $\bar{N}(T)$ is constant over each plateau, but between adjacent plateaus changes by a single spike per burst. Each plateau is labeled by its respective value of $\bar{N}(T)$, and the transition

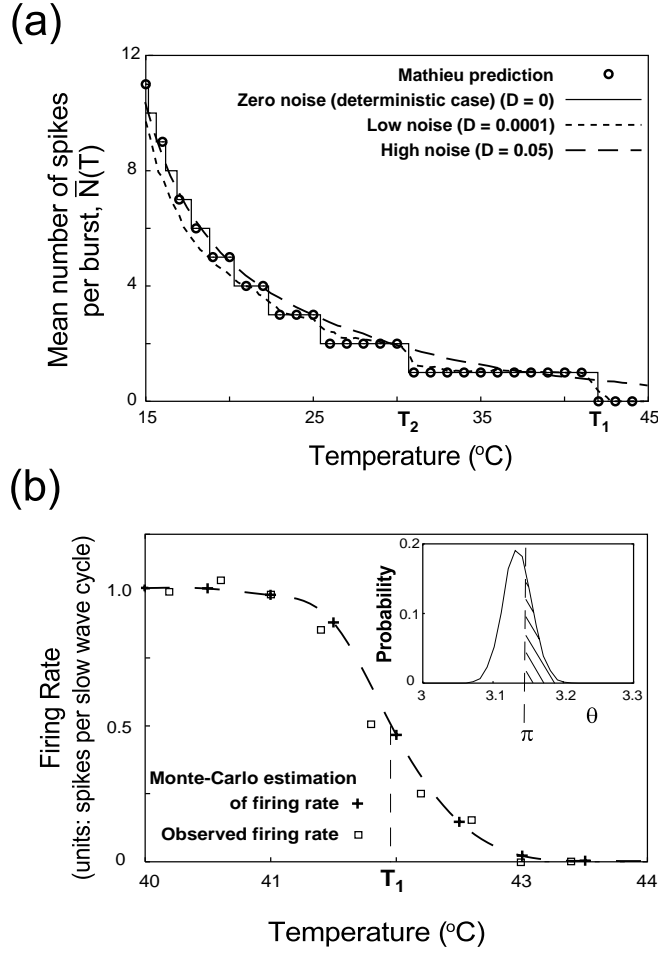


Figure 5: (a) Mean number of action potentials per burst, \bar{N} , versus temperature, T . Simulation results with several noise levels are shown; the circles mark the corresponding Mathieu predictions for the deterministic neuron. (b) Monte Carlo estimation of the firing rate close to the transition temperature T_1 for $D = 10^{-4}$. The squares show numerically observed firing rates (measured in spikes per slow wave cycle), and the crosses depict the Monte Carlo approximation to rate as estimated by the method of section 4.2 (the dashed curve is a spline fit through these data points). The inset figure shows a Monte Carlo approximation to the probability density $p(\theta, t = \pi/\Omega|\hat{\theta}_s, 0)$ at $T = 42^{\circ}\text{C}$. Parameters are: $A_0 = 0.3$, $A_T = 0.001$, $b_0 = 0.675$, $b_T = 0.007$, $\Omega_0 = -\pi/150$, and $\Omega_T = \pi/1500$.

temperature between the n th and $(n - 1)$ th plateaus by T_n . If a low level of noise is now introduced, the staircase retains its shape but the steps become rounded; as D increases, the plateaus disappear, and $\bar{N}(T)$ approaches a smoothly decreasing function of temperature.

To understand the origin of the staircase, we reinterpret equation 3.11 as a gradient system in the limit of high friction:

$$\frac{d\theta}{dt} = -\frac{dU}{d\theta} + \xi(t). \quad (4.1)$$

We now view our model as a particle obeying a noisy dynamics in a time-dependent potential $U(\theta, t)$ of the form

$$U(\theta, t) = -\gamma(t) [\lambda(t)\theta + \sin(\theta)], \quad (4.2)$$

where

$$\gamma(t) = 1 + A \cos(\Omega t) \quad \text{and} \quad \lambda(t) = \frac{b - A \cos(\Omega t)}{1 + A \cos(\Omega t)}, \quad (4.3)$$

which is equivalent to an active rotator with periodic coefficients. The multiplicative term $\gamma(t)$ periodically rescales the magnitude of U , while $\lambda(t)$ periodically sculpts the shape of U (see Figure 6). The coefficients $\gamma(t)$ and $\lambda(t)$ are both periodic with period $2\pi/\Omega$ but are antiphase.

4.1 The Deterministic Limit ($D \rightarrow 0$): the Strutt Map. At any time t , the bias $\lambda(t)$ characterizes the instantaneous deterministic dynamics. Three regimes occur:

1. $\lambda(t) < 1$. The oscillator has one stable and one unstable fixed point, each given by the solutions to $\theta = \cos^{-1}(-\lambda)$. This is termed the *locked state*, and the dynamics relaxes to the stable fixed point (see the inset to Figure 6a).
2. $\lambda(t) = 1$. The stable and unstable fixed points coalesce via a saddle-node bifurcation to form a half-stable fixed point at $\theta = \pi$.
3. $\lambda(t) > 1$. The potential U has no minima and the deterministic dynamics has no fixed points. The oscillator therefore rotates with the variable velocity

$$\dot{\theta}(t) = \gamma(t) (\lambda(t) + \cos(\theta)), \quad (4.4)$$

and each rotation corresponds to the firing of an action potential. Such a solution is termed a *running state* (see the inset to Figure 6b).

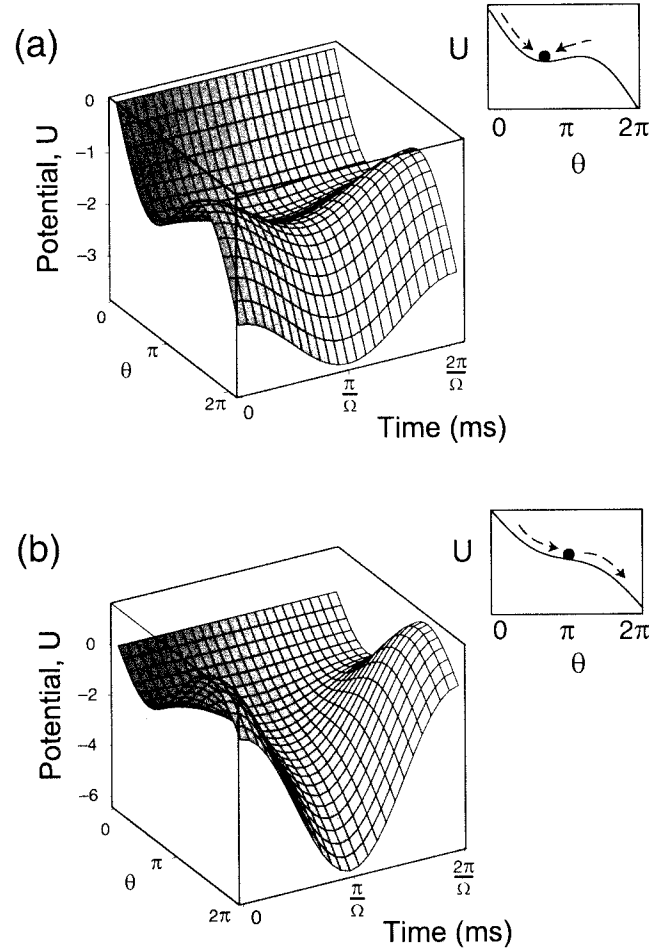


Figure 6: The potential $U(\theta, t)$ for a single cycle of the slow wave. (a) $\lambda_{\max} < 1$, the always-stable potential. For low noise levels the oscillator tends to remain close to the minima of the potential. (b) $\lambda_{\max} > 1, \lambda_{\min} < 1$, the partially stable potential. When the barrier is absent, the oscillator may escape beyond 2π , generating an action potential. The particle is then reinjected at $\theta = 0$. The inset figures caricature the respective potentials at times $t = (2n + 1)\pi/\Omega, n \in \mathbb{Z}$.

Thus the extremal values of $\lambda(t)$, $\lambda_{\max} = (b + A)/(1 - A)$ and $\lambda_{\min} = (b - A)/(1 + A)$, define the global behavior of the system:

1. $\lambda_{\min} > 1$. The potential U never has a barrier. The neuron fires regularly, and the system is always unstable.
2. $\lambda_{\max} < 1$. The potential always has a finite barrier. The neuron is quiescent, and the system is always stable.
3. $\lambda_{\min} < 1$ and $\lambda_{\max} > 1$. A potential barrier exists for part of the cycle, and the system is partially stable.

An always-unstable system spikes repetitively at a very high rate. It therefore has no useful temporal structure, and so no relevance to our study. We therefore choose A_0 and A_T such that at low temperatures, the system is partially stable, and at high temperatures the system is always stable. We denote the critical temperature for which $\lambda_{\max} = 1$ by T_c , which is defined by

$$b(T_c) + A(T_c) = 1 - A(T_c) \quad (4.5)$$

and so, for the linear system (see equation 3.9),

$$T_c = \frac{1 - b_0 - 2A_0}{2A_T - b_T} \quad (4.6)$$

(for the coefficients shown in Figures 3 and 5, $T_c = 55^\circ\text{C}$). We therefore see that the n th burst plateau corresponds to a partially stable system for which the time when the barrier is absent is commensurate with the time to wind n times round the torus.

Perhaps surprisingly it is found that $T_1 < T_c$ (recall that T_1 is the temperature beyond which the deterministic neuron ceases firing). In fact, there is a finite temperature range between T_1 and T_c for which one would expect the running mode to persist over a significant part of the oscillation period even though, in the limit $D \rightarrow 0$, no spikes are generated. This is a consequence of critical slowing down close to the bifurcation. If λ_{\max} is only marginally greater than unity, then a “ghost” of the half-stable fixed point causes the relaxation time τ_0 to become comparable to the slow-wave oscillation period. The system is then unable to escape beyond this laminar region before λ decreases again below unity and the system goes through the saddle-node bifurcation in reverse.

We may in fact derive a condition for beating to occur. For at least one action potential to be generated per oscillation, θ must pass through π (i.e., passes the point at which the stable and unstable fixed points collide) within the first half of the cycle—within $\tau_0 < \pi/\Omega$. If θ passes through π after one cycle, then it moves so slowly that it is unable to escape before the bifurcation

recurs, and it becomes trapped by the barrier. Thus, if the oscillator is found at the stable state, $\hat{\theta}_s \equiv \cos^{-1}(-\lambda_{\min})$, at $t = 0$, then we have the condition

$$\int_0^{\frac{\pi}{\Omega}} \dot{\theta} dt \geq \pi - \hat{\theta}_s. \quad (4.7)$$

The envelope function (recall equation 3.8) is a heuristic that loosely predicts how the deterministic pattern varies with temperature. However, for this deterministic case, it is possible to predict exactly how many action potentials are actually generated during one cycle. Following Ermentrout and Kopell (1986) we recast the zero-noise limit of equation 3.11 as a Mathieu equation. We use the transformation

$$\frac{1}{V} \frac{d}{dt} V = \frac{1+b}{2} \cot\left(\frac{\theta}{2}\right) \quad (4.8)$$

and simple trigonometric identities to obtain

$$\frac{d^2}{ds^2} V + [a - 2q \cos(2s)] V = 0, \quad (4.9)$$

where we have rescaled time so that $2s = \Omega t$ and introduced, to accord with convention (McLachlan, 1947), the coefficients a and q

$$a = \frac{b^2 - 1}{\Omega^2} \quad \text{and} \quad q = \frac{A(b+1)}{\Omega^2}. \quad (4.10)$$

The Mathieu equation (4.9), is a linear equation with periodic coefficients (McLachlan, 1947), and hence (according to Floquet's theorem) has a general solution of the form

$$V(s) = c_1 \exp(\rho_1 s) p_1(s) + c_2 \exp(\rho_2 s) p_2(s), \quad (4.11)$$

where c_1 and c_2 are constants, ρ_1 and ρ_2 are termed characteristic exponents, and the $p_i(s)$ are periodic functions with the same minimal period as the periodic coefficient of the original equation, 4.9. When the ρ_i are pure imaginary (and conjugate), the solutions are bounded and oscillatory. However, when both are real (with $\rho_1 = -\rho_2$), all solutions are unbounded. The (a, q) plane divides into a countable set of simply connected regions for which either all solutions fall into the former class—the stable regions—or belong to the latter class—the unstable regions. This situation is depicted in the Strutt stability map (see Figure 7) (McLachlan, 1947).

Let I_j denote the j th instability tongue of the Strutt map, which corresponds to a set of general solutions with real exponents. Unbounded solutions are generally of one of two qualitative types (Nayfeh & Mook, 1995):

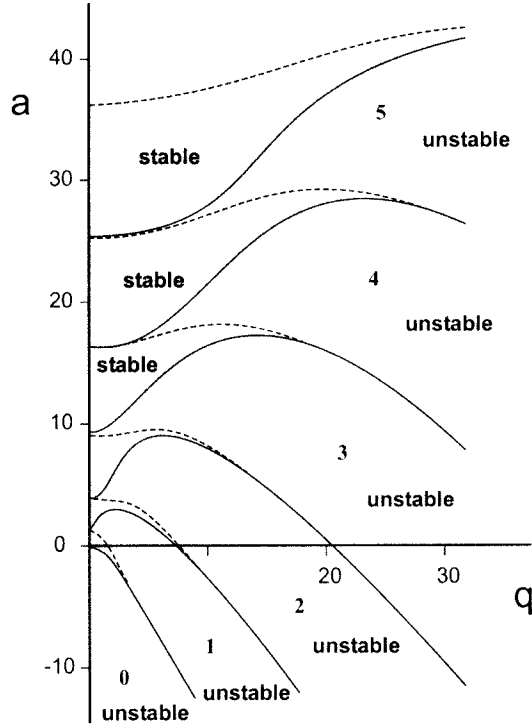


Figure 7: The Strutt map: stability and instability regimes for the Mathieu equation. The graph is symmetric about the ordinate. The j th instability tongue represents an area of parameter space in which the neuron bursts (fires repetitively with a periodic pattern), and with a burst containing j spikes.

either oscillatory but with an amplitude that increases exponentially with time, or nonoscillatory but exponentially increasing. Our interest is with the former. According to the Sturm oscillation theorem (Coddington & Levinson, 1955), each of the periodic functions, $p_1(s)$ and $p_2(s)$, of a solution in the j th instability region has exactly j zeros per oscillation period of the slow wave (Ermentrout & Kopell, 1986).

Returning to our original variable,

$$\theta(s) = 2 \cot^{-1} \left[\frac{2(c_1(\alpha p_1(s) + p_1'(s)) + c_2 \exp[-2\alpha s](-\alpha p_2(s) + p_2'(s)))}{(1+b)(c_1 p_1(s) + c_2 \exp[-2\alpha s] p_2(s))} \right], \quad (4.12)$$

since $\alpha > 0$, then if $c_1 \neq 0$, $\theta(s)$ exponentially approaches the stable periodic solution

$$\theta_s(s) = 2 \cot^{-1} \left[\frac{2(\alpha p_1(s) + p_1'(s))}{p_1(s)(1+b)} \right]. \quad (4.13)$$

Since $p_1(s)$ has j zeros over the period of the slow-wave oscillation, the argument to \cot^{-1} “blows up” j times over this period. Consequently θ passes 0 j times within a period. Furthermore, by use of equations 3.5 and 3.7, it is simple to verify that each time θ passes through 0, it does so with a positive velocity. Thus, θ wraps around the torus j times per slow-wave cycle, and this then corresponds to a burst containing j spikes.

The coefficients of the Mathieu equation, 4.9, are parameterized by the temperature, and so as T varies, it carves a trajectory across the (a, q) plane. As the trajectory passes through the k th instability region, the neuron has a burst length of k spikes, generating the plateaus seen in Figure 5.

Note also that while ε appears in the EK transform, it drops out of the canonical model (see equation 3.2). Ermentrout and Kopell further show (1986, lemma 4) that for any pair of Mathieu coefficients (a, q) that lie in any instability region of the Strutt map, there exists a sufficiently small ε such that there is a solution to the full equations that converges to the reduced one.

4.2 Stochastic Dynamics of Bursting and Beating.

4.2.1 Smoothing the Mathieu Staircase. To clarify how the transitions between plateaus become smoothed as noise is introduced, we will examine the transition from beating to quiescence, occurring at $T = T_1$. Our conclusions will extrapolate to each transition between the n th and $(n - 1)$ th plateaus.

We introduce a small amount of noise into the dynamics of equation 3.11, so that $D \neq 0$.³ For T marginally greater than T_1 , the neuron now emits a succession of single spikes that are entrained to the underlying slow wave, but occasionally cycles are skipped. As the temperature increases beyond T_1 , cycles are skipped more frequently, until the neuron becomes silent. At any T , the skipping rate depends on the noise intensity; the noise simply propels the voltage over the unstable fixed point (Gang, Ditzinger, Ning, & Haken, 1993; Rappel & Strogatz, 1994).

Conversely, for temperatures slightly below T_1 the noisy neuron is seen to misfire occasionally and thus skip a period of the slow-wave oscillation. In this regime, although the deterministic neuron is able to fire, the noise can trap the system above the ghost bottleneck and postpone its firing. To understand this, note that critical slowing down in the laminar bottleneck means

³ Recall equation 3.10; the noise intensity is assumed to be independent of T .

that the noisy dynamics have negligible deterministic motion (“drift”) in this region and so approximates a one-dimensional Wiener process. Thus, the neuron is equally likely to diffuse in either direction. If the diffusion acts to diminish $\dot{\theta}$, the firing condition in equation 4.7 may be violated and firing retarded. Qualitatively similar retardation and trapping due to noise has been noted by Apostolico et al. (1994) as a failure mechanism in bistable switches.

These two skipping modes have a natural interpretation in terms of the Strutt map. Neural dynamics close to a transition temperature correspond to a region in parameter space that is close to a tongue boundary. The inclusion of noise allows the neuron to execute a random walk through the Strutt map, and so to explore adjacent regions of the parameter space. Thus, if the neuron is in the j th tongue but lies close to the $(j + 1)$ th, then the noise can carry the neuron over the boundary, and thus augment the burst. Conversely, if the neuron lies closer to the boundary with the $(j - 1)$ th tongue, the noise can delete a spike from the burst.

4.2.2 The Skipping Rate. We have seen that for the deterministic neuron, a spike is generated only if θ passes through π within the first half of the cycle. Numerical investigations of equation 4.1 show that the condition in equation 4.7 generalizes to the case of weak noise, provided we consider instead the probability that θ is greater than π after half a driving period. We introduce the conditional probability density $p(\theta, t|\theta_0, t_0)$ subject to the initial condition

$$p(\theta, 0|\hat{\theta}_s, 0) = \delta(\theta - \hat{\theta}_s) \quad (4.14)$$

(recall that the stable state $\hat{\theta}_s \equiv \cos^{-1}(-\lambda_{\min})$). Therefore the probability $P(\theta > \pi, t|\hat{\theta}_s, 0)$ that at a time t , θ is greater than π is given by

$$P(\theta > \pi, t|\hat{\theta}_s, 0) = \int_{\pi}^{2\pi} p(\theta, t|\hat{\theta}_s, 0)d\theta, \quad (4.15)$$

which is equal to the probability of generating an action potential. By performing an ensemble average, we may equate this quantity with the mean number of spikes per slow-wave cycle.

The conditional probability density obeys a Smoluchowski equation (Risken, 1989),

$$\frac{\partial}{\partial t} p(\theta, t|\hat{\theta}_s, 0) = \frac{\partial}{\partial \theta} \left[U'(\theta, t) + \frac{D}{2} \frac{\partial}{\partial \theta} \right] p(\theta, t|\hat{\theta}_s, 0) \quad (4.16)$$

where $U'(\theta, t)$ represents the spatial derivative of the potential. The time dependence of the potential forbids a general closed solution to equation 4.16 and furthermore makes a numerical solution difficult to obtain. However,

a Monte Carlo approximation to the probability density $p(\theta, t|\hat{\theta}_s, 0)$ may be obtained. We first numerically iterate an ensemble of \mathcal{N} receptors $\theta_i(t)$, $i = 1, \dots, \mathcal{N}$, for half of one slow-wave period, subject to the initial condition $\theta_i(t = 0) = \hat{\theta}_s \equiv \cos^{-1}(-\lambda_{\min})$, $\forall i \in \mathcal{N}$. An approximation to $p(\theta, t|\hat{\theta}_s, 0)$ will be given by a normalized histogram of the ensemble of $\theta_i(t = \pi/\Omega)$ and so an estimation of the firing rate may be found from equation 4.15 (see Figure 5).

5 Discussion

We have developed a phase model of slow-wave parabolic bursting cold receptors that qualitatively reproduces the observed firing patterns at different constant temperatures. The stochastic extension of this model accounts for the variability in the number of spikes per burst and for the skipping patterns. Our analysis in terms of a Strutt map allows a description of the regions of parameter space that produce specific firing patterns, in both the deterministic and noise-driven regimes. It is worthwhile to make a few points regarding our model.

5.1 Paths for Other Receptors. There are many different thermally responsive bursting cells (Braun et al., 1984), for example, the feline lingual and infraorbital nerves, the boa constrictor warm fiber, and the dogfish ampullae of Lorenzini. The discharge patterns of all of these cell types exhibit many similar qualitative features, but quantitatively they differ; for example, they have differing burst lengths at a given temperature. In addition, there can also be considerable variation within a single cell type (recall section 2). Therefore, the paradigm of a temperature-dependent noisy trajectory through the Strutt map allows a universal model that might help to explain the discharge patterns of more of these cells.

5.2 Chaos. The existence of chaos in thermoresponsive neuronal spike-trains has been recently studied in both real (Braun et al., 1997) and model (Longtin & Hinzer, 1996) neurons. However, the phase model reported here does not support chaos; instead its spike-train irregularities have a stochastic origin. Is this important? For this class of neurons at least, the answer is “probably not,” since it is more likely that the bursting pattern itself is the fundamental carrier of information rather than the timing of individual spikes within a burst. Such patterns may be more reliably detected by higher neurons due to synaptic facilitation.

5.3 Additive Versus Multiplicative Noise. We introduced thermal and pump noise as a simple, additive term on the θ dynamics. However, there are other ways in which noise might enter the dynamical equations. Consider instead an additive term, $\xi_s(t)$, on the slow dynamics (see also Gutkin &

Ermentrout, 1998), so that equation 3.5 becomes

$$\begin{aligned}\frac{d\theta}{dt} &= [b + \cos(\theta)] - [1 - \cos(\theta)] [A \cos(\Omega t) + \xi_s(t)] \\ &= F(\theta, t) - [1 - \cos(\theta)] \xi_s(t).\end{aligned}\tag{5.1}$$

$\xi_s(t)$ now couples multiplicatively to the fast dynamics, and when $\theta = 0$, the effect of noise vanishes. Since the noise cannot carry the system around the limit cycle, it might therefore appear that this sort of noise cannot contribute to the spiking dynamics. However, recall the gradient system (see equation 4.1) and Figure 6, and note that $\theta = 0$ is halfway down a fairly steep slope. At this time (the peak amplitude of a fast sodium spike) and for the noise levels considered here, the deterministic dynamics dominate and carry the cell around the limit cycle. The additive noise introduced in equation 3.11 would also have very little impact at this time.⁴ Further, following Sigeti (1988), we could replace $[1 - \cos(\theta)] \xi_s(t)$ by a mean noise (Gutkin & Ermentrout, 1998), averaged over some spatial domain (say, between the stable and unstable fixed points), and still get quantitatively similar behavior.

5.4 Different Noise Distribution. In the absence of any electrophysiological motivation, we have introduced a white noise process. Recall that the discharge pattern derives from a random walk through the Strutt map and that spike augmentation and deletion arise when the random walk crosses a tongue boundary. In consequence, we note that other additive noise distributions (such as the Ornstein–Uhlenbeck process considered in Longtin & Hinzer, 1996) will produce qualitatively similar burst patterns, and so the actual noise distribution is not pertinent to an understanding of the general model. However, the choice of noise distribution will be extremely important when describing a specific burst pattern.

5.5 Asymmetric Burst Patterns and Parabolicity. In contrast to our phase model, discharge patterns from real cold receptors exhibit asymmetric burst patterns. Typical (Braun et al., 1980) burst profiles comprise a rapid increase followed by a slower decrease in spike frequency, resulting in a sawtooth profile. However, parabolic cells generally exhibit burst profiles with firing rates that vary nonmonotonically throughout the burst. Thus, definitively labeling the discharge of these cells as parabolic is problematic. However, according to Rinzel and Lee (1987), the symmetry of the discharge of the Plant model can be manipulated by parameter modification. Furthermore,

⁴ For additive noise, there is in fact a finite probability for θ to recross zero in the opposite direction. However, such an event is unlikely, and, moreover, simply crossing zero does not constitute a spike. A spike is a full rotation around the limit cycle, and the probability that this will happen is vanishingly small (at least for these noise levels).

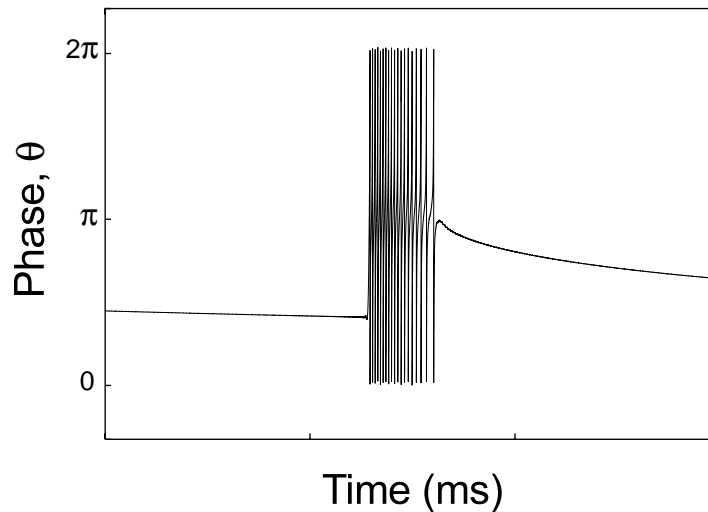


Figure 8: A burst pattern from a sawtooth slow wave (the first few terms of the expansion $A[1 - \sum_n \frac{1}{n} \sin(nx)]$). Parameters are $\Omega = 0.001$, $A = 0.5$, and $b = 0.6$ (cf. figure 1 of Braun et al., 1980). See also Ermentrout and Kopell (1986).

for our canonical model, the time-dependent term $A \cos(\Omega t)$ models the oscillatory slow-wave dynamics. We have no electrophysiological guidelines to direct our choice for its functional form, and so we have chosen a cosine for its analytical tractability. However, the asymmetry of the discharge of real cells suggests that if the bursting is of slow-wave type, then the wave is asymmetric. Thus a more complex waveform may better reproduce the finer details of the discharge pattern. Figure 8 shows a single burst driven by a sawtooth slow wave, and the finer details of this pattern are in better agreement with data (compare with Figure 1 of Braun et al., 1980). Our analysis readily extends to slow waves of this form, except now the Mathieu equation must be replaced by a more general Hill equation (Ermentrout & Kopell, 1986).

6 Conclusions

We have presented a tractable phase model for cold-receptor function. Our phase model can be related to more complex, biophysical models of neuronal operation, and we have shown how certain parameters of the phase model derive from Plant's ionic model. We have investigated the phase model, both numerically and analytically, in the deterministic regime and also when subject to a finite amount of thermal noise. Numerically obtained

spike trains and interspike interval histograms from the phase model agree well with the experimental data. From our investigations, we have shown that skipping might be caused by noise. We have further shown that both the number of spikes in a burst and also the skipping rate at any given temperature may be predicted. Finally, we have studied how altering the noise level affects the dynamics and shown that the skipping regime may be subdivided. The first part of skipping is caused by noise-induced trapping, and the second by noise-induced spiking. Our findings provide a framework in which to study the effect of various physicochemical parameters in the environment of these receptors and analytical insight into the variability of patterns across receptors.

Appendix

Here we analyze the temperature dependence of the slow-wave frequency in a model of cold receptors based on the Plant model described in Longtin and Hinzer (1996). This model is five-dimensional and possesses a clear separation of timescales as discussed in (Rinzel & Lee, 1987). The three fast variables are the voltage V and the gating variables h and n of the fast-spiking dynamics (sodium inactivation and potassium activation). The slow variables are the gating variable x of the slow inward current and the intracellular calcium concentration y . The dynamics of V are given by

$$C_m \frac{dV}{dt} = -I_{ion}(V, h, n; x, y). \quad (\text{A.1})$$

The dynamics of x and y are given by

$$\frac{dx}{dt} = \lambda [x_{\infty}(V) - x] / \tau_x \quad (\text{A.2})$$

$$\frac{dy}{dt} = \rho [K_c x (V_{Ca} - V) - y]. \quad (\text{A.3})$$

In the approximation where the full system can be separated into fast and slow subsystems, the slow dynamics are

$$\frac{dx}{dt} = \lambda [x_{\infty}(V_{ss}) - x] / \tau_x \quad (\text{A.4})$$

$$\frac{dy}{dt} = \rho [K_c x (V_{Ca} - V_{ss}) - y], \quad (\text{A.5})$$

where V_{ss} is the pseudo-steady-state membrane voltage, obtained as a solution of

$$0 = I_{ion}(V_{ss}, h_{\infty}(V_{ss}), n_{\infty}(V_{ss}); x, y). \quad (\text{A.6})$$

The important fact is that $V_{ss} = V_{ss}(x, y)$. Hence, the (x, y) dynamics are coupled together by V_{ss} . Based on numerical computations of this surface in the absence of fast-spiking dynamics (Rinzel & Lee, 1987; see in particular Figure 2), we then approximate the pseudo-steady-state surface by the plane

$$V_{ss}(x, y) \approx V_o + a_1x + a_2y, \quad (\text{A.7})$$

where V_o is the mean value of the slow-wave potential, and the partial derivatives a_1 and a_2 are constants. These constants are negative according to (Rinzel & Lee, 1987; see Figure 2). Using this form for V_{ss} , we can write

$$x_\infty^{-1}(x, y) = \exp[0.15(-50 - V_o - a_1x - a_2y)] + 1. \quad (\text{A.8})$$

Introducing the coordinates $X \equiv x - x^*$ and $Y \equiv y - y^*$, the linearization about the fixed point (x^*, y^*) of this two-dimensional subsystem is

$$\frac{dX}{dt} = \alpha\lambda X + \beta\lambda Y \quad (\text{A.9})$$

$$\frac{dY}{dt} = \gamma\rho X + \delta\rho Y, \quad (\text{A.10})$$

where we have isolated the temperature-dependent parameters λ and ρ from the other parameters:

$$\alpha \equiv \left(\frac{\partial x_\infty}{\partial x} \Big|_{x^*, y^*} - 1 \right) \tau_x^{-1} \quad (\text{A.11})$$

$$\beta \equiv \tau_x^{-1} \frac{\partial x_\infty}{\partial y} \Big|_{x^*, y^*} \quad (\text{A.12})$$

$$\gamma \equiv K_c(V_{Ca} - V_o - 2a_1x^* - a_2y^*) \quad (\text{A.13})$$

$$\delta \equiv -(K_c a_2 x^* + 1). \quad (\text{A.14})$$

We note that x and y are positive quantities, as is δ ; α and β are negative, and the sign of δ is dependent on precise parameter values. If $(\alpha\lambda + \rho\delta)^2 < 4\rho\lambda(\alpha\delta - \gamma\beta)$, the eigenvalues are complex. At the bifurcation point, $\alpha\lambda + \rho\delta = 0$ and the frequency is given by

$$\omega_H = \sqrt{(\alpha\delta - \gamma\beta)\rho\lambda} \sim (\rho\lambda)^{1/2}, \quad (\text{A.15})$$

which is real since $\alpha\delta - \gamma\beta > 0$.

Acknowledgments

This work was supported by a Loughborough University postgraduate studentship, a traveling fellowship from the John Phillips Guest fund, and NSERC (Canada).

References

- Apostolico, F., Gammaitoni, L., Marchesoni, F., & Santucci S. (1994). Resonant trapping: A failure mechanism in switch transitions. *Physical Review E*, 55(1), 36–39.
- Braun, H. A., Bade, H., & Hensel, H. (1980). Static, dynamic discharge patterns of bursting cold fibres related to hypothetical receptor mechanisms. *Pflügers Archiv—European Journal of Physiology*, 386, 1–9.
- Braun, H. A., Huber, M. T., Dewald, M., Schäfer, K., & Voigt, K. (1998). Computer simulations of neuronal signal transduction: The role of nonlinear dynamics and noise. *International Journal of Bifurcation and Chaos*, 8(5), 881–889.
- Braun, H. A., Schäfer, K., Voigt, K., Peters, R., Bretschneider, F., Pei, X., Wilkens, L., & Moss, F. (1997). Low-dimensional dynamics in sensory biology 1: Thermally sensitive electroreceptors of the catfish. *Journal of Computational Neuroscience*, 4, 335–347.
- Braun, H. A., Schäfer, K., & Wissing, H. (1990). Theories and models of temperature transduction. In J. Bligh & K. Voigt (Eds.), *Thermoreception and thermal regulation* (pp. 18–29). Berlin: Springer-Verlag.
- Braun, H. A., Schäfer, K., Wissing, H., & Hensel H. (1984). Periodic transduction processes in thermosensitive receptors. In W. Hamman & A. Iggo (Eds.), *Sensory receptor mechanisms* (pp. 147–156). Singapore: World Scientific Publishing.
- Braun, H. A., Wissing, H., Schäfer, K., & Hirsch, M. C. (1994). Oscillation and noise determine signal transduction in shark multimodal sensory cells. *Nature*, 367, 270–273.
- Canavier, C. C., Clark, J. W., & Byrne, J. H. (1991). Simulation of the bursting activity of neuron R15 in *Aplysia*: Role of ion currents, calcium balance, modulatory transmitters. *Journal of Neurophysiology*, 66, 2107–2124.
- Carpenter, D. O. (1967). Temperature effects on pacemaker generation, membrane potential, and critical firing threshold in *Aplysia* neurons. *Journal of General Physiology*, 50(6), 1469–1484.
- Coddington, E. A., & Levinson, N. (1955). *Theory of ordinary differential equations*. New York: McGraw-Hill.
- DeFelice, L. J. (1981). *Introduction to membrane noise*. New York: Plenum.
- Dykes, R. W. (1975). Coding of steady, transient temperatures by cutaneous “cold” fibers serving the hand of monkeys. *Biophysical Journal*, 98, 485–500.
- Ermentrout, G. B., & Kopell, N. (1986). Parabolic bursting in an excitable system coupled with a slow oscillation. *SIAM Journal of Applied Mathematics*, 46(2), 233–253.
- Gang, H., Ditzinger, T., Ning, C. Z., & Haken, H. (1993). Stochastic resonance without external periodic force. *Physical Review Letters*, 71(6), 807–810.
- Gutkin, B. S., & Ermentrout, G. B. (1998). Dynamics of membrane excitability determine interspike interval variability: A link between spike generation mechanisms and cortical spike train statistics. *Neural Computation*, 10, 1047–1065.

- Ivanov, K. P. (1990). The location, function of different skin thermoreceptors. In J. Bligh & K. Voigt (Eds.), *Thermoreception and thermal regulation* (pp. 37–43). Berlin: Springer-Verlag.
- Kopell, N., & Ermentrout, G. B. (1986). Subcellular oscillations and bursting. *Mathematical Biosciences*, 78, 265–291.
- Lisman, J. E. (1997). Bursts as a reliable unit of neural information: Making unreliable synapses reliable. *Trends in Neuroscience*, 20(1), 38–43.
- Longtin, A., & Hinzer, K. (1996). Encoding with bursting, subthreshold oscillations, and noise in mammalian cold receptors. *Neural Computation*, 8, 215–255.
- McLachlan, N. W. (1947). *Theory and application of Mathieu functions*. Oxford: Clarendon Press.
- Nayfeh, A. H., & Mook, D. T. (1995). *Nonlinear oscillations*. New York: Wiley.
- Plant, R. E. (1981). Bifurcation and resonance in a model for bursting nerve-cells. *Journal of Mathematical Biology*, 11(15), 15–32.
- Rappel, W., & Strogatz, S. H. (1994). Stochastic resonance in an autonomous system with a nonuniform limit cycle. *Physical Review E*, 50(4), 3249–3250.
- Rinzel, J., & Lee, Y. S. (1987). Dissection of a model for neuronal parabolic bursting. *Journal of Mathematical Biology*, 25, 653–675.
- Risken, H. (1989). *The Fokker-Planck equation* (2nd ed.). New York: Springer-Verlag.
- Schäfer, K., Braun, H. A., & Rempe, L. (1988). Classification of a calcium conductance in cold receptors. *Progress in Brain Research*, 74, 29–36.
- Schäfer, K., Braun, H. A., & Rempe, L. (1990). Mechanisms of sensory transduction in cold receptors. In J. Bligh & K. Voigt (Eds.), *Thermoreception and thermal regulation* (pp. 30–36). Berlin: Springer-Verlag.
- Sigeti, D. E. (1988). *Universal results for the effects of noise on dynamical systems*. Unpublished doctoral dissertation, University of Texas at Austin.
- Soto-Treviño, C., Kopell, N., & Watson, D. (1996). Parabolic bursting revisited. *Journal of Mathematical Biology*, 35, 114–128.
- Strogatz, S. H. (1994). *Nonlinear dynamics and chaos*. Reading, MA: Addison-Wesley.
- Wiederhold, M. L., & Carpenter, D. O. (1982). Possible role of pacemaker mechanisms in sensory systems. In D. O. Carpenter (Ed.), *Cellular pacemakers* (Vol. 2, pp. 27–58). New York: Wiley-Interscience.
- Willis, J. A., Gaubatz, G. L., & Carpenter, D. O. (1974). The role of the electrogenic pump in modulation of pacemaker discharge of *Aplysia* neurons. *Journal of Cellular Physiology*, 84, 463–471.